Chinese Journal of Mechanical Engineering

ORIGINAL ARTICLE

Open Access

Time Synchronous Averaging Based on Cross-power Spectrum

Ling Wang[1], Minghui Hu[1,2*], Bo Ma[1] and Zhinong Jiang[1,2]

Abstract

Periodic components are of great significance for fault diagnosis and health monitoring of rotating machinery. Time synchronous averaging is an effective and convenient technique for extracting those components. However, the performance of time synchronous averaging is seriously limited when the separate segments are poorly synchronized. This paper proposes a new averaging method capable of extracting periodic components without external reference and an accurate period to solve this problem. With this approach, phase detection and compensation eliminate all segments' phase differences, which enables the segments to be well synchronized. The effectiveness of the proposed method is validated by numerical and experimental signals.

Keywords Time synchronous averaging, Phase detection, Cross-power spectrum, Fault diagnosis

1 Introduction

Time synchronous averaging (TSA) is a powerful technique that extracts periodic components from a composite signal [1–5]. It is widely used in noise reduction and fault diagnosis [6–10]. In this method, segments separated by the exact period are averaged. Any component not synchronous with this period will be attenuated [11–13].

It is known that TSA works well only if all the segments are synchronized. Generally, an external trigger signal, provided by a tachometer, is used for synchronous sampling. This external reference signal should be stable so that effective synchronization can be obtained [14]. However, in some cases, installing a tachometer is difficult or impossible. If there is no reference signal available, it is necessary to estimate the fundamental frequency of the components to be extracted [15, 16]. While in practice, accurate estimation of the fundamental frequency is quite hard, and the rounding error needs to be considered [17].

There are many studies to improve the performance of TSA. Bonnardot et al. proposed a method for angular resampling by using the acceleration signal of a gearbox [18]. On this basis, an automatic TSA method was proposed, whose effectiveness depends on the local signal-to-noise ratio of mesh harmonics [19]. The time domain average scanning was presented to extract periodic components when no external reference signal exists. The fundamental frequency is obtained by searching within the possible range [20]. This optimization process can be adaptive [21]. Halim et al. combined TSA and wavelet transform to synchronize the data with the rotation period based on the reference peak [22]. Wu et al. eliminated the phase error by fractional delay filtering, but this method requires an accurate estimation of the fundamental frequency [23]. Guo et al. screened all segments according to the correlation coefficient, providing a new research route [24].

The above discussion indicates that TSA requires effective synchronization of segments. Therefore, this paper proposes time synchronous averaging based on the

*Correspondence:
Minghui Hu
humh2008@163.com
[1] Key Laboratory of Engine Health Monitoring-control and Networking of Ministry of Education, Beijing University of Chemical Technology, Beijing 100029, China
[2] Beijing Key Laboratory of High-end Mechanical Equipment Health Monitoring and Self-Recovery, Beijing University of Chemical Technology, Beijing 100029, China

cross-power spectrum to cope with the current challenges. First, the original vibration signal is divided into equal-length segments. Then the phases of the segments are calculated and compensated, which means that the phase differences are eliminated. Finally, the synchronized segments are averaged. Numerical and experimental signals are presented to verify the proposed method.

This paper is organized as follows. Section 2 reviews the theory of time synchronous averaging, and Section 3 introduces the proposed method in detail. Section 4 studies the performance of the proposed method by numerical simulation. In Section 5, the experimental signal is provided for validating the proposed method. Section 6 shows the conclusions.

2 Time Synchronous Averaging

The basic theory of TSA is as follows. $x(t)$ represents the original vibration signal of rotating machinery. Its discrete sequence can be expressed as $x(n)(n = 0, 1, 2, \cdots)$, where $x(n)$ is equivalent to $x(n\Delta t)$. Δt denotes the sampling interval. The expression of TSA is

$$\begin{cases} y(n) = \dfrac{1}{N}\displaystyle\sum_{r=0}^{N-1} x(n + rM), \\ n = 0, 1, \cdots, M - 1, \end{cases} \tag{1}$$

where $y(n)$ is the average signal, N is the number of segments, and M is the number of sampling points per segment.

The frequency response function of Eq. (1) can be expressed as:

$$H(f) = \frac{1}{N}\frac{\sin(\pi N f/f_0)}{\sin(\pi f/f_0)}\exp(-j\pi(N-1)f/f_0), \tag{2}$$

where f_0 is the fundamental frequency of the periodic components.

As illustrated in Figure 1, the typical shape of the frequency response function is like a comb. Therefore, TSA works like a comb filter with main lobes centered around integer multiples of the fundamental frequency. It is easy to find that the periodic components are unchanged, while the nonsynchronous components and noise are attenuated.

An external reference signal is usually needed to get the desired result. However, when no reference signal is available, TSA's performance will be limited by rounding and frequency estimation errors. The phase error caused by them can be expressed as:

$$\psi_{r,m} \approx 2\pi mr\Delta M\frac{f_0}{f_s} + 2\pi mr\frac{\Delta f}{f_o}, \tag{3}$$

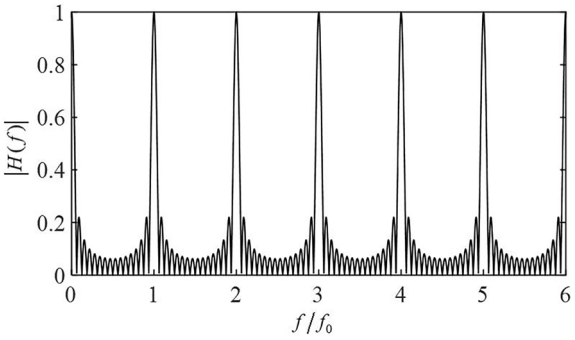

Figure 1 Frequency response of TSA

where m is the order of the component, ΔM is the rounding error, Δf is the frequency estimation error, and f_s is the sampling frequency.

It has been proved that the phase error will lead to a sharp attenuation of the periodic components. Detailed analyses can be found in Refs. [17, 20, 23].

3 Time Synchronous Averaging Based on Cross-Power Spectrum

3.1 Phase Detection Based on Cross-power Spectrum

For continuous signals $x(t)$ and $y(t)$, the expression of their cross-correlation function is:

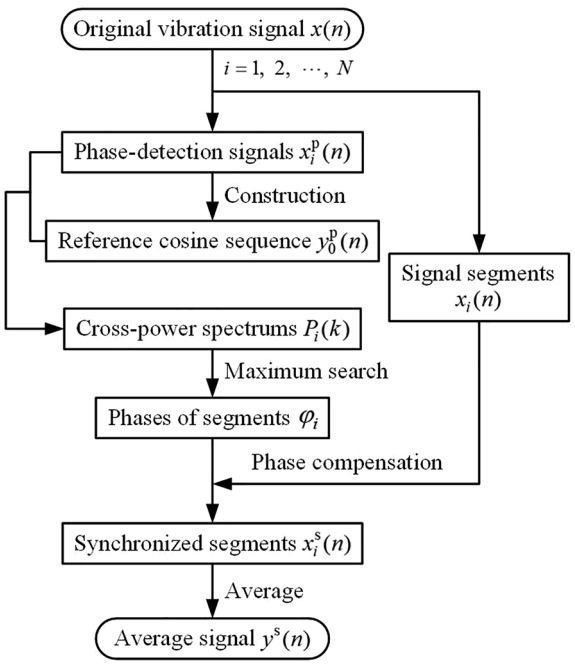

Figure 2 Flowchart of the proposed method

Table 1 Amplitudes of the simulated signal

Parameter	A_1	A_3	$A_{3.5}$	A_5	$A_{5.7}$	A_6	A_8
Value	0.5	0.8	0.6	0.4	0.3	0.6	0.5

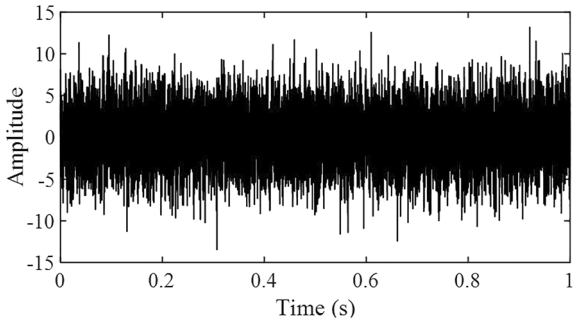

Figure 3 Simulated signal

$$R(\tau) = \int_{-\infty}^{+\infty} x(t)\, y(t-\tau)\mathrm{d}t, \tag{4}$$

where τ is the delay.

This function is mainly used to reflect the correlation of two different signals. After cross-correlation, components with the same frequency are enhanced, retaining the phase information, while the others get suppressed. Thus, the signal components of interest can be enhanced in this way. A phase-detection method based on the cross-power spectrum is introduced next.

To detect the phase of the fundamental component in the discrete vibration signal $x(n)$, a reference cosine sequence is constructed as:

$$y_0(n) = \cos(2\pi f_0 n). \tag{5}$$

According to the definition of convolution, the cross-correlation function can be expressed as:

$$R(n) = x(n) * y_0(-n), \tag{6}$$

where $*$ denotes the convolution.

With the Fourier transform and time-domain convolution theorem, the cross-power spectrum can be calculated as:

$$P(k) = X(k)Y_0^*(k), \tag{7}$$

where $Y_0^*(k)$ represents the complex conjugation of $Y_0(k)$; $X(k)$ and $Y_0(k)$ represent the discrete Fourier transforms of $x(n)$ and $y_0(n)$, respectively.

The fundamental component in the vibration signal is thus enhanced. Its phase φ is equal to that of a complex

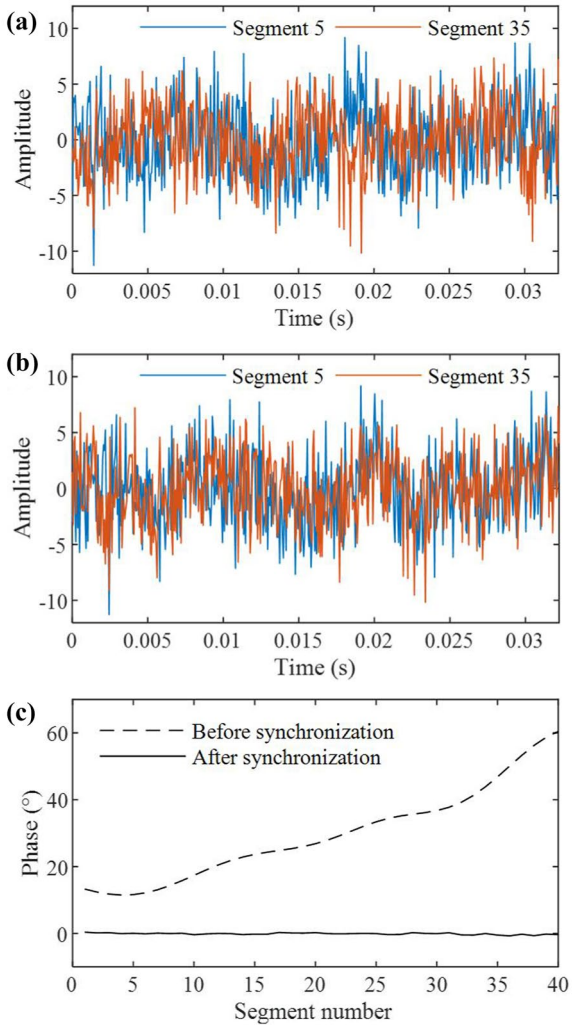

Figure 4 **a** Unsynchronized segments, **b** synchronized segments, **c** phases of all segments

number at the maximum amplitude of the cross-power spectrum. The expression is:

$$\begin{cases} \varphi = \arg(P(k_0)), \\ \left|P(k_0)\right| = \max\limits_{0<k<\pi f_s} \left(\left|P(k)\right|\right). \end{cases} \tag{8}$$

This method strengthens the fundamental component through cross-correlation operation and extracts the phase from the cross-power spectrum. It has the advantages of strong adaptability, high precision, and small

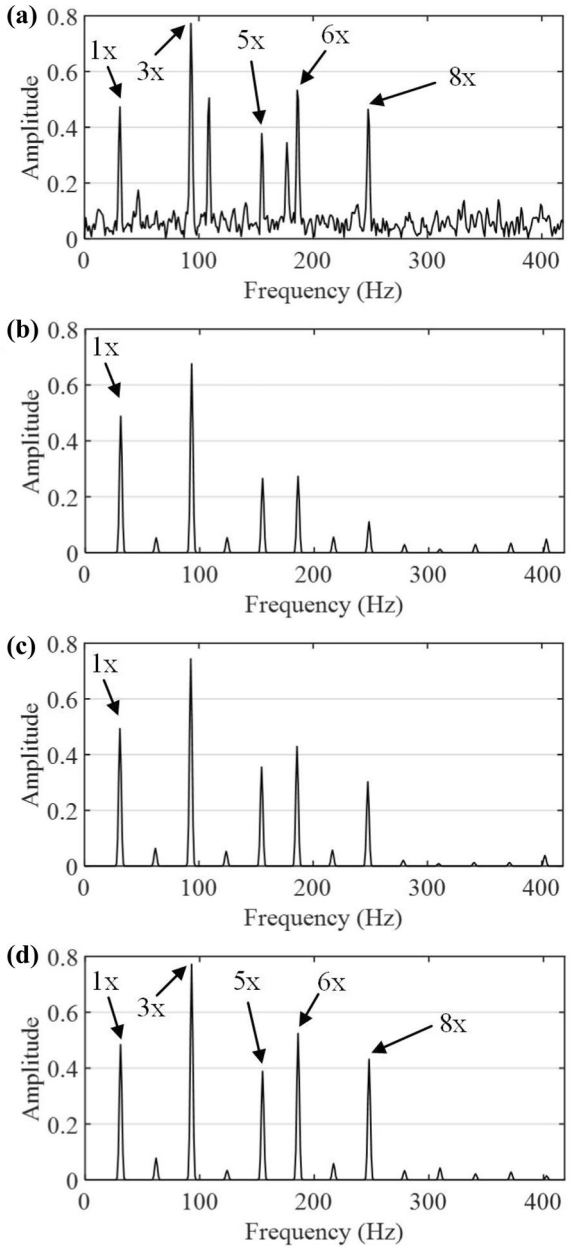

Figure 5 Spectrum comparison: **a** Simulated signal, **b** Method 1, **c** Method 2, **d** Method 3

computation [25]. In addition, there is no limitation on the component of interest.

3.2 The Proposed Method

The detailed procedure of the proposed method can be divided into five steps, as shown in Figure 2.

Step 1: Some separate segments are obtained from the original signal by continuous and equispaced

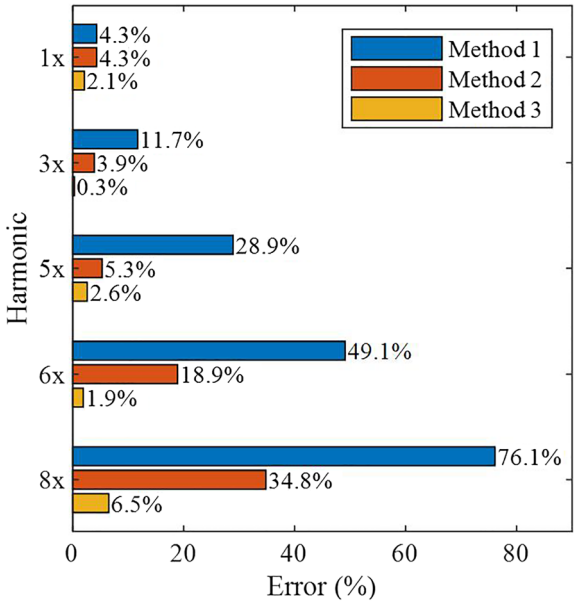

Figure 6 Amplitude errors of the three methods

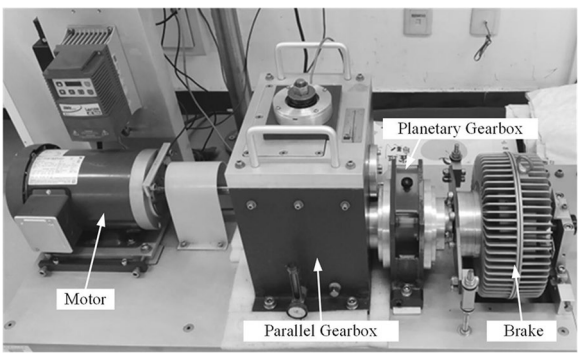

Figure 7 Gearbox test bench

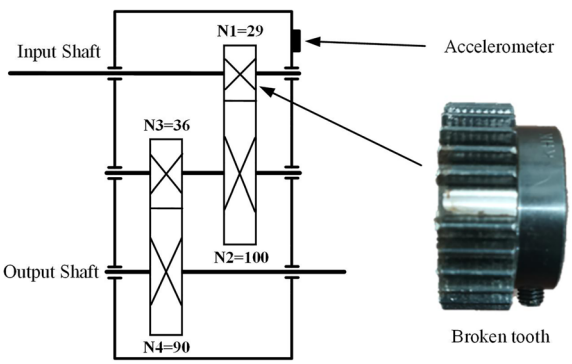

Figure 8 Parallel gearbox and broken gear

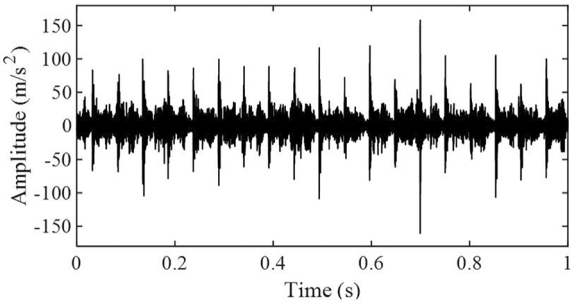

Figure 9 Experimental signal

interception. The ith $(i = 1, 2, \cdots, N)$ segment can be expressed as:

$$\begin{cases} x_i(n) = x[n + (i-1)M], \\ n = 0, 1, \cdots, M-1, \end{cases} \tag{9}$$

where $M = \text{round}(f_s/f_0)$.

Step 2: The phase-detection signal of the ith segment can be defined as:

$$\begin{cases} x_i^{\text{p}}(n) = x[n + (i-1)M], \\ n = 0, 1, \cdots, f_s - 1. \end{cases} \tag{10}$$

Step 3: The reference cosine sequence $y_0^{\text{p}}(n)$, corresponding to the phase-detection signal obtained in Step 2, is constructed by Eq. (5). Then the cross-power spectrum $P_i(k)$ is calculated according to Eq. (7). Finally, the phase φ_i can be calculated by Eq. (8). It will be used for phase compensation.

Step 4: The phase obtained in Step 3 is converted to the number of sampling points. The expression is:

$$N_i = \text{round}\left(\frac{\varphi_i}{2\pi f_0} f_s\right). \tag{11}$$

The phase differences among segments are eliminated by cyclic shift. This process can be expressed as follows:

$$x_i^{\text{s}}(n) = \begin{cases} x_i(n + M - N_i), n < N_i, \\ x_i(n - N_i), n \geq N_i, \\ n = 0, 1, \cdots, M-1, \end{cases} \tag{12}$$

where $x_i^{\text{s}}(n)$ is the ith synchronized segment.

Step 5: All the synchronized segments are averaged.

$$y^{\text{s}}(n) = \frac{1}{N} \sum_{i=1}^{N} x_i^{\text{s}}(n), \tag{13}$$

where $y^{\text{s}}(n)$ is the average signal of the proposed method.

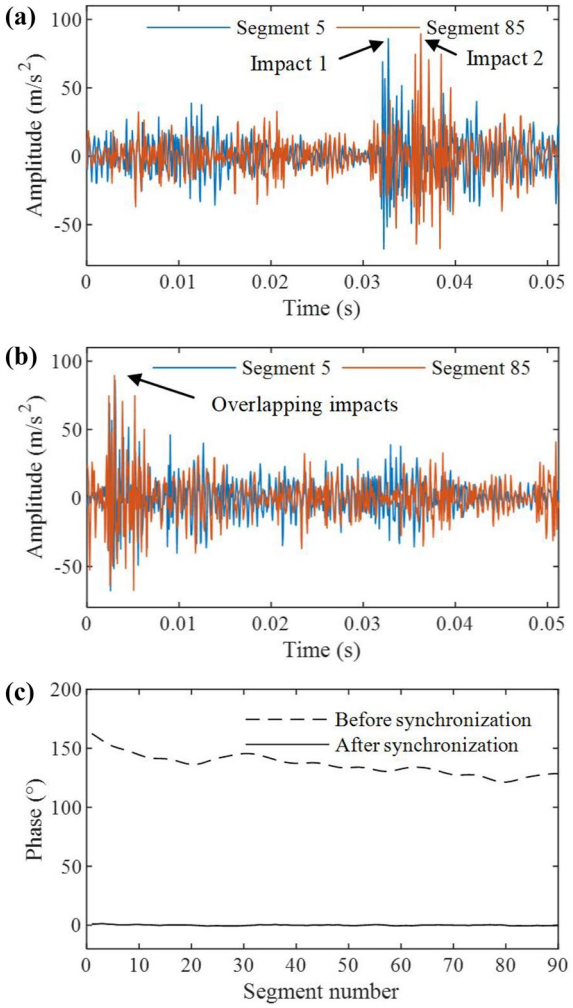

Figure 10 **a** Unsynchronized segments, **b** Synchronized segments, **c** Phases of all segments

4 Numerical Simulation

In this section, a numerical simulation is given to test the performance of the proposed method. Two existing TSA methods are introduced for comparison. They are original TSA (Method 1) and TSA based on a fractional delay filter (Method 2) proposed by Wu et al. [23]. The simulated signal comprises periodic components, non-synchronous components, and noise. The expression is:

$$\begin{cases} x(t) = \sum_k A_k \cos(2\pi k f_0 t + \varphi_k) + n(t), \\ k = 1, 3, 3.5, 5, 5.7, 6, 8, \end{cases} \tag{14}$$

where $n(t)$ is the noise signal; A_k and φ_k are the amplitude and initial phase of the signal component with frequency kf_0, respectively. Amplitudes are shown in Table 1, while initial phases can be set to any value. f_0=31.05 Hz, and the sampling frequency is 16384 Hz.

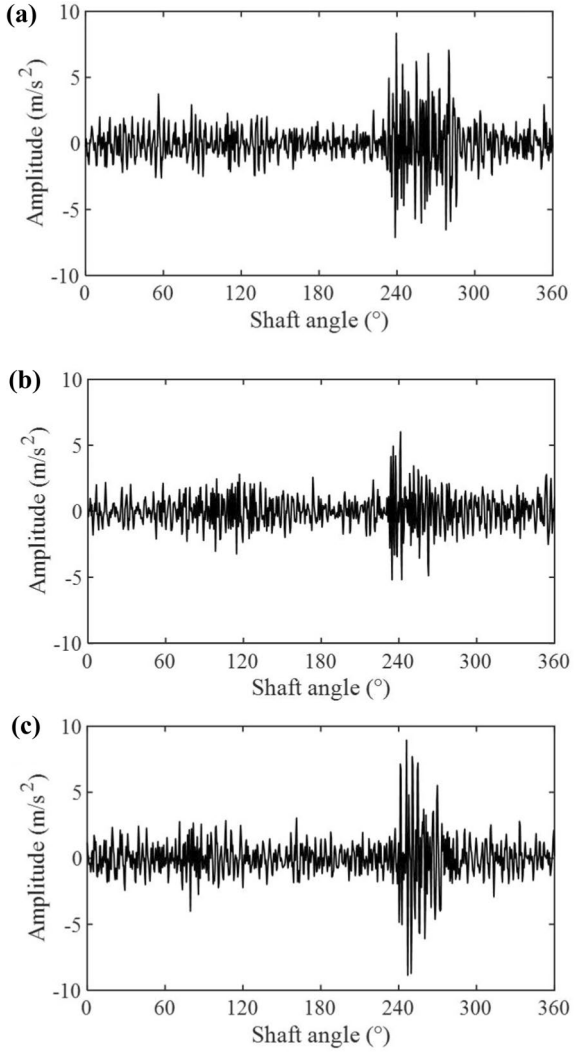

Figure 11 Average waveforms: **a** Method 1, **b** Method 2, **c** Method 3

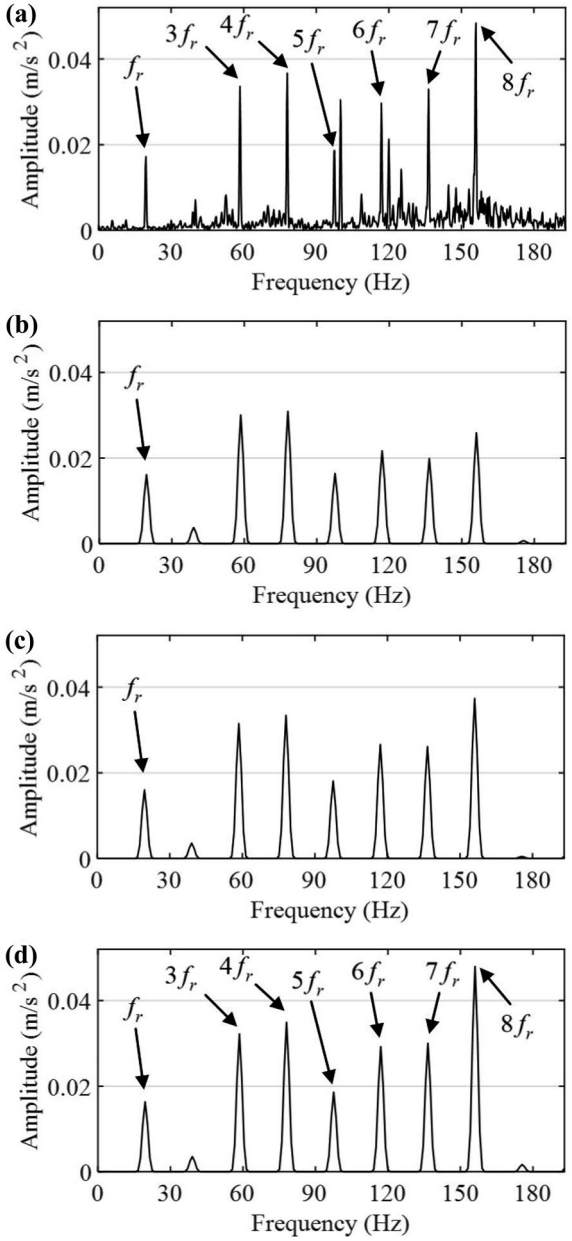

Figure 12 Spectrum comparison: **a** experimental signal, **b** Method 1, **c** Method 2, **d** Method 3

The waveform of the simulated signal is shown in Figure 3.

The frequency estimation error in actual situations should be considered, and the fundamental frequency of the simulated signal is estimated to be 31 Hz. The number of sampling points per segment is rounded to 529, and 40 segments are obtained by continuous interception.

The waveforms of segments 5 and 35 are shown in Figure 4(a). It can be observed that the two segments are not well synchronized. Figure 4(b) shows that the two segments almost overlap after phase detection and compensation.

The phase before synchronization increases with the segment number, as shown in Figure 4(c). The maximum value is about 60°, leading to a sharp attenuation of the average result. After synchronization, all phases are stable around 0°, which means that the phase differences are eliminated.

Figure 5(a) shows the simulated signal in the frequency domain. The results of the three methods are shown in Figure 5(b)–(d). It is easy to find that the amplitudes of some harmonics in the results of Method 1 and Method 2 are obviously attenuated.

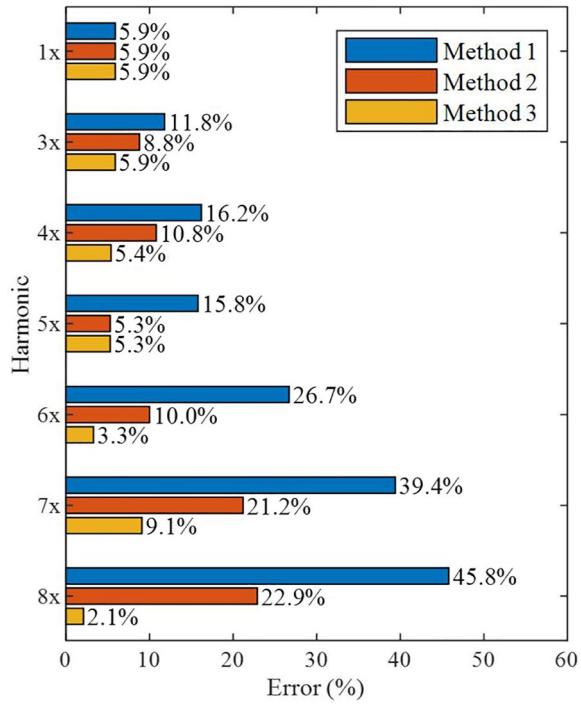

Figure 13 Amplitude errors of the three methods

Figure 6 gives the amplitude errors of the three methods based on Figure 5. It can be observed that the errors of Method 3 are the smallest.

5 Experimental Validation

5.1 Set-up of the Experiment

We apply the proposed method to analyze the test-bench signal for further validation. The test bench is mainly composed of a motor, a parallel gearbox, a planetary gearbox, and a magnetic brake, as illustrated in Figure 7.

In this experiment, a gear with one broken tooth is installed in the parallel gearbox to simulate the gear fault. The structure of the parallel gearbox and the fault gear are shown in Figure 8. B&K PULSE is used for data acquisition, and the accelerometer is PCB 608A11. The accelerometer is located on the housing of the parallel gearbox. Considering the requirement of frequency bandwidth, the convenience of calculating the time for spectrum analysis, and preset options for the instrument, we select the sampling frequency as 16384 Hz [26, 27]. The rotation speed of the motor is 1200 r/min. By searching in the frequency domain, the fundamental frequency of the input shaft is estimated to be 19.5 Hz.

5.2 Analysis of the Experimental Signal

The waveform of the experimental signal is shown in Figure 9, from which impacts caused by gear fault can be observed.

For the experimental signal, the number of sampling points per segment is rounded to 840, and 90 segments are obtained by continuous interception. The waveforms of segments 5 and 85 are shown in Figure 10(a). It can be found that there is an impact in both segments, which is consistent with the fault feature. At the same time, it should also be noted that there is an obvious phase difference between the two impacts. Figure 10(b) shows the waveforms of the two segments after phase detection and compensation. They almost overlap.

As shown in Figure 10(c), the phase differences after synchronization are close to 0°, which means that the segments are well synchronized.

Once a gear tooth is damaged, an impulsive vibration per revolution will be generated. As a result, detecting periodic impacts is a practical method for gear fault diagnosis.

Figure 11 shows the average waveforms of the three methods. It can be seen from Figure 11(c) that impacts appear once in a gear revolution, which indicates the presence of the gear fault. In contrast, the fault-induced impacts in the average waveforms of Method 1 and Method 2 are not strong enough. The gear fault is easier to be identified by the proposed method.

Figure 12(a) shows the spectrum of the experimental signal. Frequency components unrelated to gear fault can be misleading in fault diagnosis.

The spectrum results of the three methods are shown in Figure 12(b)–(d). The characteristic frequency of the gear fault and its harmonics can be clearly observed in Figure 12(d). Although these components can also be found from other two methods, they are severely attenuated.

As shown in Figure 13, the amplitude errors of the three methods are calculated. The result of Method 1 is the worst, and the amplitude error of 8x is as high as 45.8%. Due to the frequency estimation error, Method 2 can not reach the theoretical efficiency. Its maximum error is 22.9%. The maximum amplitude error of Method 3 is only 9.1%, which shows the superiority of the proposed method in extracting periodic components.

6 Conclusions

(1) A novel TSA method that is capable of synchronizing the separate segments without an external reference signal is proposed in this paper.
(2) In numerical and experimental validations, the segments are well synchronized by the pro-

posed method, and the periodic components are extracted.

(3) Compared with other methods, the amplitude attenuation of the proposed method is less. The superiority of the proposed method in extracting periodic components with limited frequency estimation error is thus reflected.

Acknowledgements
Not applicable.

Author contributions
MH was in charge of the whole trial; LW wrote the manuscript; BM and ZJ assisted with sampling and laboratory analyses. All authors read and approved the final manuscript.

Authors' information
Ling Wang, born in 1998, is currently a master candidate at *Key Laboratory of Engine Health Monitoring-Control and Networking of Ministry of Education, Beijing University of Chemical Technology, China*. He received his bachelor degree from *Beijing University of Chemical Technology, China*, in 2020. His research interests include fault diagnosis and signal processing.
Minghui Hu, born in 1990, is currently an associate professor at *Beijing University of Chemical Technology, China*. He received his PhD degree from *Beijing University of Chemical Technology, China*, in 2018. His research interests include condition monitoring and fault diagnosis of aircraft engine.
Bo Ma, born in 1977, is currently a professor at *Beijing University of Chemical Technology, China*. He received his PhD degree from *Beijing University of Chemical Technology, China*, in 2006. His research interests include intelligent fault diagnosis and machine vision.
Zhinong Jiang, born in 1967, is currently a professor at *Beijing University of Chemical Technology, China*. He received his PhD degree from *Beijing University of Chemical Technology, China*, in 2010. His research interests include condition monitoring and fault diagnosis of high-end mechanical equipment.

Funding
Supported by National Postdoctoral Program for Innovative Talent of China (Grant No. BX20180031).

Data availability
Not applicable.

Competing interests
The authors declare no competing financial interests.

Received: 9 September 2022 Revised: 23 February 2023 Accepted: 27 February 2023
Published online: 11 April 2023

References

[1]. Y G Lei, Z J He, J Lin, et al. Research advances of fault diagnosis technique for planetary gearboxes. *Journal of Mechanical Engineering*, 2011, 47(19): 59-67. (in Chinese)
[2]. H K Li, X T Lian, S Zhou. Application on weak information classification by using wavelet scalogram synchronous averaging. *Journal of Mechanical Engineering*, 2013, 49(5): 32-38. (in Chinese)
[3]. N Ahamed, Y Pandya, A Parey. Spur gear tooth root crack detection using time synchronous averaging under fluctuating speed. *Measurement*, 2014, 52(1): 1-11.
[4]. W D Mark. Time-synchronous-averaging of gear-meshing-vibration transducer responses for elimination of harmonic contributions from the mating gear and the gear pair. *Mechanical Systems and Signal Processing*, 2015, 62: 21-29.
[5]. I Bravo-Imaz, H D Ardakani, Z C Liu, et al. Motor current signature analysis for gearbox condition monitoring under transient speeds using wavelet analysis and dual-level time synchronous averaging. *Mechanical Systems and Signal Processing*, 2017, 94: 73-84.
[6]. L Zhang, N Q Hu. Time domain synchronous moving average and its application to gear fault detection. *IEEE Access*, 2019, 7: 93035-93048.
[7]. K L Wu, Y Xing, N Chu, et al. A carrier wave extraction method for cavitation characterization based on time synchronous average and time-frequency analysis. *Journal of Sound and Vibration*, 2020, 489: 115682.
[8] W Y Wang, K Johnson, T Galati. Vibration analysis of planet gear bore-rim failure using enhanced planet time synchronous averaging. *Engineering Failure Analysis*, 2020, 117: 104942.
[9] X Laval, C Mailhes, N Martin, et al. Amplitude and phase interaction in Hilbert demodulation of vibration signals: Natural gear wear modeling and time tracking for condition monitoring. *Mechanical Systems and Signal Processing*, 2021, 150: 107321.
[10] X K Yang, M J Zuo, Z G Tian. Development of crack induced impulse-based condition indicators for early tooth crack severity assessment. Mechanical Systems and Signal Processing, 2022: 165
[11] S Braun. The extraction of periodic waveforms by time domain averaging. *Acta Acustica United with Acustica*, 1975, 32(2): 69-77.
[12] P D McFadden. Interpolation techniques for time domain averaging of gear vibration. *Mechanical Systems and Signal Processing*, 1989, 3(1): 87-97.
[13] S Braun. The synchronous (time domain) average revisited. *Mechanical Systems and Signal Processing*, 2011, 25(4): 1087-1102.
[14] V Camerini, G Coppotelli, S Bendisch, et al. Impact of pulse time uncertainty on synchronous average: Statistical analysis and relevance to rotating machinery diagnosis. *Mechanical Systems and Signal Processing*, 2019, 129: 308-336.
[15] S Braun, B Seth. Analysis of repetitive mechanism signatures. *Journal of Sound and Vibration*, 1980, 70(4): 513-526.
[16] M Feder. Parameter estimation and extraction of helicopter signals observed with a wide-band interference. *IEEE Transactions on Signal Processing*, 1993, 41(1): 232.
[17] G J Shen, L M Tao, Y C Xu. Research on phase error accumulation effect of time synchronous averaging. *Journal of Vibration Engineering*, 2007, 20(4): 335-339. (in Chinese)
[18] F Bonnardot, M E Badaoui, R B Randall, et al. Use of the acceleration signal of a gearbox in order to perform angular resampling (with limited speed fluctuation). *Mechanical Systems and Signal Processing*, 2004, 19(4): 766-785.
[19] F Combet, L Gelman. An automated methodology for performing time synchronous averaging of a gearbox signal without speed sensor. *Mechanical Systems and Signal Processing*, 2006, 21(6): 2590-2606.
[20] L M Zhu, H Ding, X Y Zhu. Extraction of periodic signal without external reference by time-domain average scanning. *IEEE Transactions on Industrial Electronics*, 2008, 55(2): 918-927.
[21] X Q Xu, J Lin, C Yan. Adaptive determination of fundamental frequency for direct time-domain averaging. *Measurement*, 2018, 124: 351-358.
[22] E B Halim, M A A S Choudhury, S L Shah, et al. Time domain averaging across all scales: A novel method for detection of gearbox faults. *Mechanical Systems and Signal Processing*, 2008, 22(2): 261-278.
[23] W T Wu, J Lin, S B Han, et al. Time domain averaging based on fractional delay filter. *Mechanical Systems and Signal Processing*, 2009, 23(5): 1447-1457.
[24] Y J Guo, X H Jin, Y D Wei, et al. Fault feature extraction based on improved TSA denoising and squared envelope spectrum. *Journal of Vibration Engineering*, 2021, 34(2): 402-410. (in Chinese)
[25] Z N Jiang, K Feng, J J Gao. Application of phase compensation filter to automatic balancing. *Journal of Vibration, Measurement & Diagnosis*, 2006, 26(3): 234-239. (in Chinese)
[26] J W Cooley, J W Tukey. An algorithm for the machine calculation of complex Fourier series. *Mathematics of Computation*, 1965, 19(90): 297-301.
[27] Y He, Z N Jiang, M H Hu, et al. Local maximum synchrosqueezing chirplet transform: an effective tool for strongly non-stationary signals of gas turbine. *IEEE Transactions on Instrumentation and Measurement*, 2021,70: 1-2.